VIII International Conference on Particle-Based Methods
PARTICLES 2023
U. Perego, M. Cremonesi, A. Franci (Eds)

PARTICLE-BASED FLOW SIMULATION OF MOLTEN ALUMINUM ALLOY THROUGH CASTING FILTERS

T. DEGUCHI[1], K. TAKI[1], AND Y. MAEDA[2]

[1] Graduate student, Dept. of Mechanical Engineering, Daido University

[2] Dept. of Mechanical Engineering, Daido University
10-3 Takiharu-cho, Minami-ku, Nagoya 457-8530 Japan
E-mail: y-maeda@daido-it.ac.jp , Web page: https://www.daido-it.ac.jp

Abstract: Casting defects can be predicted in advance of practice and countermeasures can be taken to improve casting quality and increase productivity. Applying the casting filters is a method of improvement methods for defects caused by unsuitable molten metal flow. Casting filters have the effect of removing inclusions in molten metal and rectifying the flow. However, specific conditions such as the type, pore size, and setting position of the casting filter are not clear. Casting filter conditions are determined by conventional empirical rules that are not theoretical. In the other view, the use of casting CAE is essential to realize front-loading for the process design process, in which casting defects are predicted in advance of practice and countermeasures are taken.

In the previous study, K. Taki et al. performed direct observation of mold filling and flow simulations passing through the casting filter. The particle-based COMINA CAE software was used for the flow simulation of molten metal in complex interior geometries in the filter. The calculations used a model of the filter that was reproduced on an X-ray CT system. To inspect the filter performance it was necessary to make a small and simplified filter model, which is called the 1/4 model of filter.

In the present study, the flow dynamics through the filter are investigated using various 1/4 models. The 1/4 model maintains permeability on the surface and porosity of volume while halving the dimensions. As a result, we succeed in reproducing the flow behaviour of molten metal when it passed through the filter by setting the particle size of molten metal to 1/16 of the filter's pore diameter. Further, we try to evaluate the performance of the filter by extending the calculation target from only the area around the filter to the entire mold. If mold filling behavior for the mold with filter could be simulated, it would be used effectively in casting geometry design and defect countermeasure.

Keywords. Casting Filter, Permeability, Mold filling, Direct observation, SPH

1 INTRODUCTION

Using casting CAE software, the casting defects can be predicted in advance of practice and countermeasures can be taken to improve casting quality and increase productivity. Casting defects can be broadly classified into those caused by the flow behaviour of mold filling and those caused by heat transfer and solidification behaviour. Countermeasures include changing casting plans and changing casting conditions. Among these, the application of a casting filters is a method to improvement defects caused by molten metal flow. There are three types of casting filters: strainer, honeycomb, and foam filters [1]-[3], as shown in Figure 1. The primary purposes for using are expected to have rectified disturbance and remove inclusions. However, the actual mechanisms of how the molten metal flows through the filter and how inclusions are removed are not precise. The specific conditions such as the type, pore size, and setting location of the casting filter are not clear and determined in accordance with the maker's guidelines.

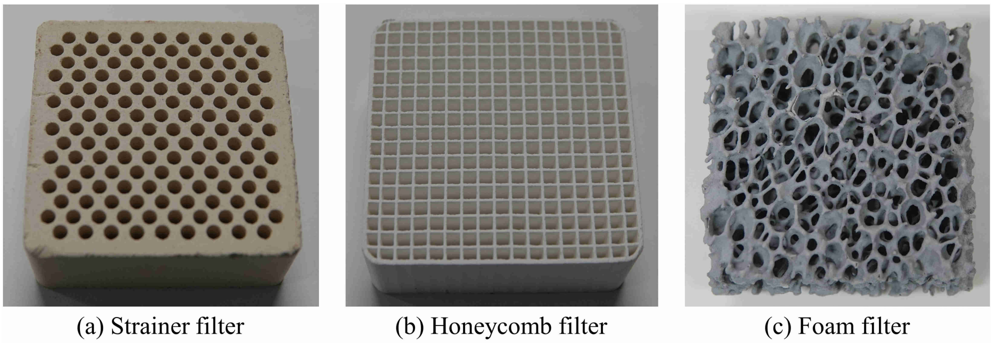

Figure 1: Three kinds of casting filter.

For research focused on the flow of molten metal passing through the filter, Yang et al.[4] investigated the distribution trends of inclusions in filters from cast iron casting experiments. Jonas Bäckman et al.[5] also investigated how different filter positions, filter roughness, filter effective cross-sectional area, and filter length affect filling using aluminum alloy. However, appropriate and specific conditions such as filter type and size are not clear. On the other hand, the use of casting CAE is essential to realize front-loading, in which casting defects are predicted in advance and countermeasures are taken. Therefore, attempts [6],[7] are being made to compare the actual phenomenon with the simulation for casting conditions without a filter.

In the previous study, K. Taki et al.[8] attempted to evaluate the performance of the filter from the visualization experiment results. However, it was difficult to evaluate filter performance with the data obtained from the experimental results, as with consideration described in the literature [4],[5]. Therefore, the casting analysis software COLNINA CAE [9],[10] was used to simulate the flow through the filter using the SPH particle method. A filter model named the 1/4 model was used to investigate filter performance, in which the dimension is halved while maintaining permeability on the surface and porosity of volume. As a result, we succeeded in reproducing the flow behaviour of molten metal when it passed through the filter by setting the particle size of molten metal to 1/16 of the filter's pore diameter. In this study investigates the effect of the initial positioning of the molten metal particles on the flow behavior of the molten metal through the filter. Further, the calculation target is extending from only the area around the filter to the entire mold to compare the flow behavior when the filter is installed.

2 CASTING PLAN AND FILTERS

2.1 Casting plan in mold filing

The casting plan of L220-Filter experimented by K. Taki et al.[8] is targeted in this study, as shown in Figure 2. The shape of the design is an L-shape with a sprue height of 220mm and a right-angle bend at the corner for a disk-like cavity with an island in the center. A filter is installed at the bottom area of the sprue. This casting design is named L220-filter.

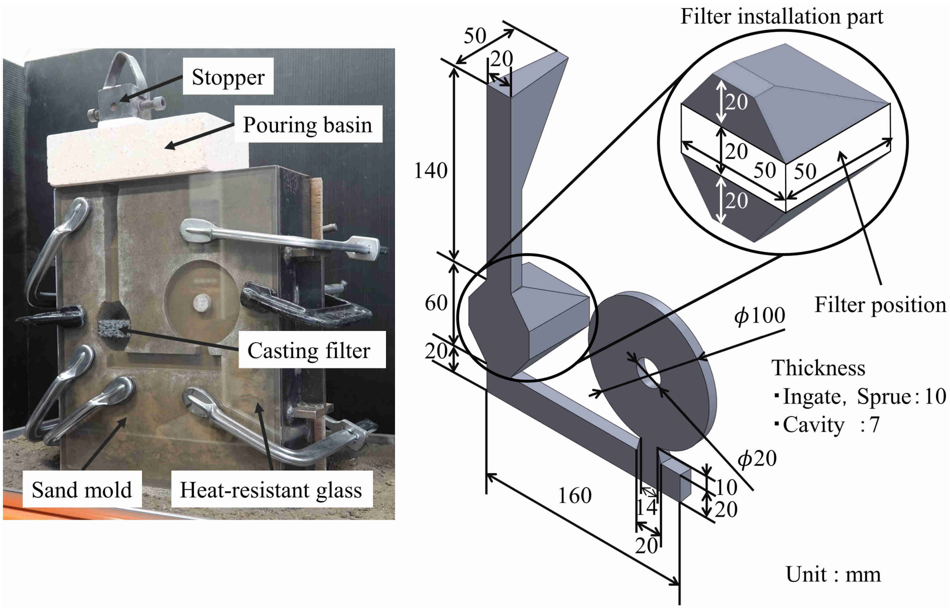

Figure 2: Overview of casting plan.

In the experiments, the molds are vertically split for direct observation, with a green sand mold on one side and heat-resistant glass on the other. To observe the flow behavior during mold filling from the front side, the end faces of the filters are aligned with the end faces of the gating design. The molten aluminum alloy Al-7%Si of an amount of 640g and a temperature of 700℃ is collected in a pouring basin in advance and flows out to the sprue in free fall by stopper release. The Flow dynamics of molten metal during mold filling are observed by a 120fps video camera in front of the mold.

2.2 Casting filters

The target filters are a foam filter with a complex shape, three honeycomb filters with square-shaped holes, and two strainer filters with round-shaped holes, for a total of six filters. The dimensions are standardized to $50mm \times 50mm$, and the filters are named foam filter 10ppi, honeycomb filter 100cpsi (cells per square inch), 200cpsi, 300cpsi, strainer filter 20t (thickness), and 12t, respectively. The filter specifications are shown in Table 1.

Permeability on the surface and porosity of volume, which are the criteria for filter evaluation, are calculated using Equations 1 and 2. Since only the structure of the foam

Table 1: Casting filter specifications. [8]

Filter Type	Size [mm]	Pore size [mm]	Number of pores [-]	Permeability on surface [%]	Porosity of volume [%]
Foam 10ppi	50 × 50 × 20	-	-	45.85	83.66
Honeycomb 100cpsi	50 × 50 × 20	□2.0	287	45.92	45.92
Honeycomb 200cpsi	50 × 50 × 20	□1.5	623	56.07	56.07
Honeycomb 300cpsi	50 × 50 × 20	□1.15	1089	57.61	57.61
Strainer 20t	50 × 50 × 20	ϕ2.7	142	32.52	32.52
Strainer 12t	50 × 50 × 12	ϕ2.5	224	43.98	43.98

filter is three-dimensionally complex, permeability on the surface is calculated from the binarization process and the porosity of volume from the Archimedes method.

$$\gamma_s = \frac{(\text{pore area}) \times (\text{number of pores})}{50 \times 50} \times 100 \tag{1}$$

$$\gamma_v = \frac{(\text{pore area}) \times (\text{number of pores}) \times (\text{thickness})}{50 \times 50 \times (\text{thickness})} \times 100 \tag{2}$$

The calculations use a model of the filter that was reproduced on an X-ray CT system, as shown in Figure 3.

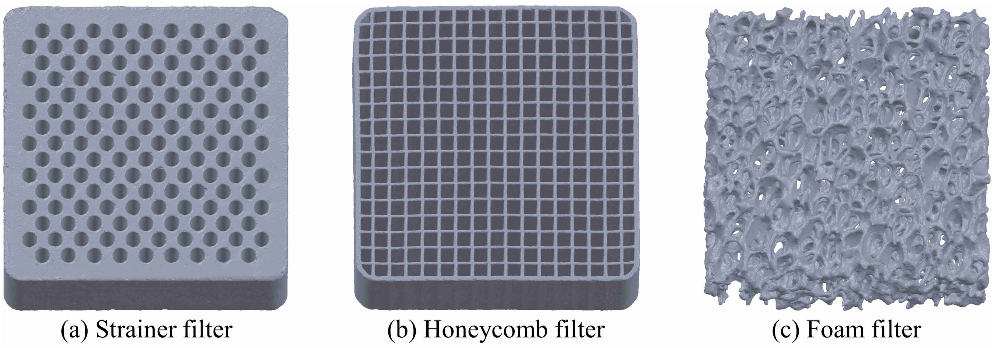

Figure 3: Calculation filter models.

3 PERFORMANCE ANALYSYS USING 1/4 MODEL

3.1 1/4 model of casting filter and calculation condition

The flow behavior during passage through the filter is calculated using particle-based SPH simulation software COLMINA CAE [9],[10]. K. Taki et al.[8] reported that the flow behavior of the calculation results showed a rough agreement with the experimental results regarding the order of filling of the sprue, runner, ingate, and cavity, although the difference in filling time. However, there was a difference in behavior during passage through the filter. The difference reason was considered to be that the molten metal particle diameter was significant about the pore diameter of the filter. So, they proposed a small and simplified filter model, which is called the 1/4 model of filter. The 1/4 model maintains permeability on the surface and porosity of volume while halving the dimensions. In the present study, the flow dynamics through the filter are investigated using various 1/4 models. Table 2 shows the specification of the 1/4 model filter.

Table 2: Specifications of 1/4 model filter.

Filter Type	Size [mm]	Pore size [mm]	Number of pores [-]	Permeability on surface [%]	Porosity of volume [%]
Foam 10ppi	25 × 25 × 10	-	-	45.85	83.66
Honeycomb 100cpsi	25 × 25 × 10	□1.49	130	45.92	45.92
Honeycomb 200cpsi	25 × 25 × 10	□1.10	289	56.07	56.07
Honeycomb 300cpsi	25 × 25 × 10	□0.86	484	57.61	57.61
Strainer 20t	25 × 25 × 10	ϕ2.01	64	32.52	32.52
Strainer 12t	25 × 25 × 6	ϕ1.87	100	43.98	43.98

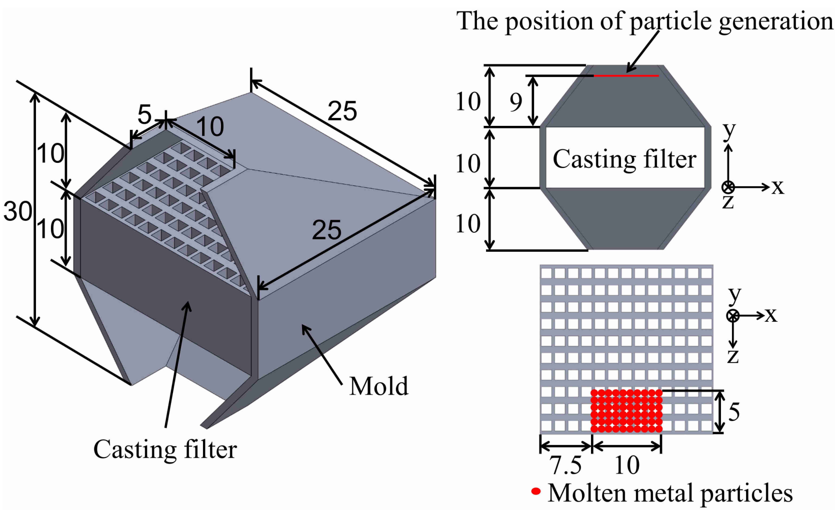

Figure 4: Performance analysis object focusing on the filter.

Figure 4 shows a performance analysis object focusing on the filter installation area, using a 1/4 model casting filter. Molten metal particles are dropped from a height of 9mm from the filter at an initial velocity of 1.2m/s. In addition to this basic model, a model is created in which the position of the filter hole was shifted by half of the hole diameter, left and right, and up and down.

Table 3 shows the calculation conditions. The molten metal particle diameters are set to 1/2, 1/4, 1/8, 1/16, and 1/32 of the filter pore diameter D, and the influence radius is 3 times the particle diameter. It uses the explicit weakly compressible SPH method.

Table 3: Calculation conditions.

Particle size [mm]	$D/2, D/4, D/8, D/16, D/32$
Influence radius	3.0 times of particle size
Parameter for sonic speed [m/s]	20

3.2 Flow behaviours during passage through the filter

For one of the calculated results, Figure 5 shows the behavior of molten aluminum alloy while passing through a honeycomb filter 100cpsi. In the experiment [8], after impacting the filter, the molten metal is divided into a flow that spreads to the left and right and a flow that passes through the pores. Applying the particle size of $dp = 1mm$ to filter with a pore size of $D = 2mm$, the molten metal particles do not spread to the left or right after impacting the filter, and appear to flow almost straight through the pores. The reason for the difference between the two flows is considered to be that the molten metal particle diameter was significant to the pore diameter of the filter.

As will be discussed later, good results can be calculated by using particles with a sufficiently small size relative to the pore size. However, if the particle diameter is reduced relative to the actual filter pore diameter, the calculation may become difficult due to particle count problems. Using the 1/4 model and particles size of $D/16$, namely the particle size of $dp = 0.093mm$ to 1/4 model filter with a pore size of $D = 1.49mm$, molten metal particles appear to be divided into a flow that spreads to the left and right after reaching the filter and a flow that passes through the pore. This behavior appears to be similar to that of the experiment.

3.3 Effect of particle size on flow behaviour during passes through filter

The percentage of particles flowing through the upper, inside, and lower of the filter at time 0.02s, a short time after the particles passed through the filter pores when it inflows at an initial velocity of 1.2m/s is investigated to the filters. Figure 6 shows the effect of particle size on filter performances obtained by using the 1/4 model filter. From the figure, the flow rate through the filter increases when the particle size is reduced relative to the pore size and it goes to the steady state. A smaller particle size than $D/16$ is adopted here because it gives reasonable results but increases the computational load.

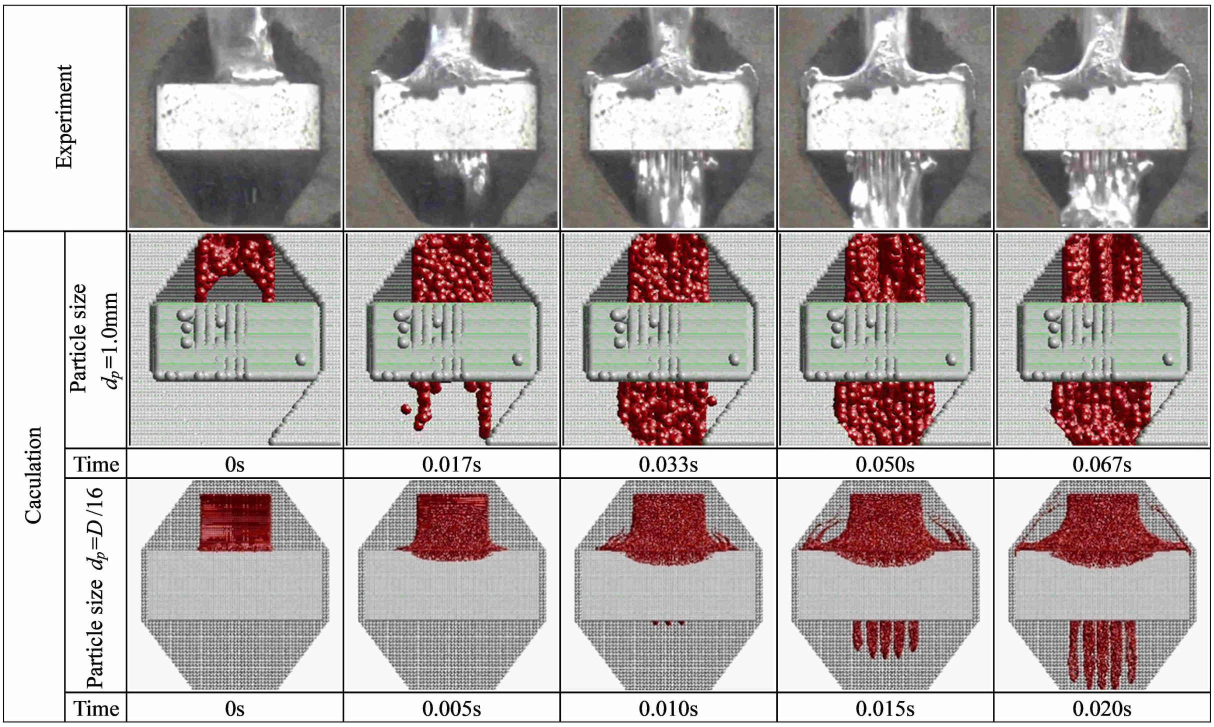

Figure 5: Flow behavior of molten aluminum alloy during passage through a honeycomb filter 100cpsi.

3.4 Influence of initial positions of particles on flow behavior

The influence of the initial positions of particles on flow behavior is investigated. Figure 7 shows three kinds of initial positions of particles. The result obtained by the condition of L1-Center is shown in Figure 6 (a). The results of L2-Horizontal and L3-Vertical are shown in Figure 8 (b) and (c), respectively. As the particle size becomes smaller, the percentage of particles in the upper of the filter decrease, while the percentage of particles in the lower of the filter increase. This trend is similar even when the initial positions of particles are changed.

4 MOLD FILLING SMULAION AND DISCUSSION

4.1 Simulation with actual size casting plan

Let us consider a simulation of the casting plan shown in Figure 2. From the above results, it is necessary to adopt a particle size smaller than 1/16 of the pore size in order to obtain suitable simulation results. In the honeycomb filter with 300cpsi, which has the maximum number of particles, the number of particles is about 700 million from a particle size of $dp = 0.07mm$ when the pore diameter is $D = 1.15mm$. Also, the number of particles with a strainer filter 20t, which is the minimum number of particles, has approximately 55 million. It may be improved in the future, but from the viewpoint of the current computer load, we think that the simulation with the actual size is not suitable.

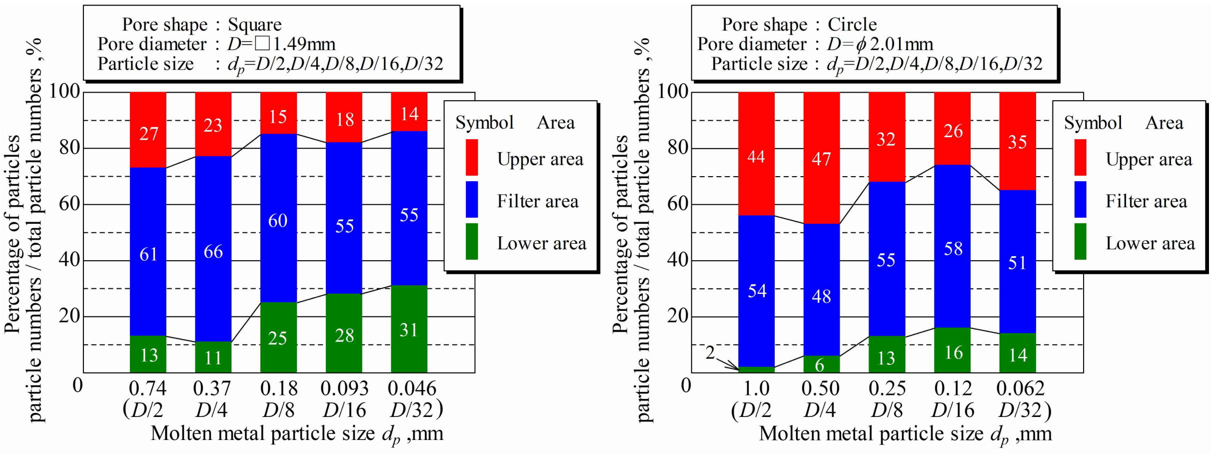

(a) Honeycomb filter 100cpsi (b) Strainer filter 20t

Figure 6: Effect of particle size on filter performances obtained by using the 1/4 model filter.

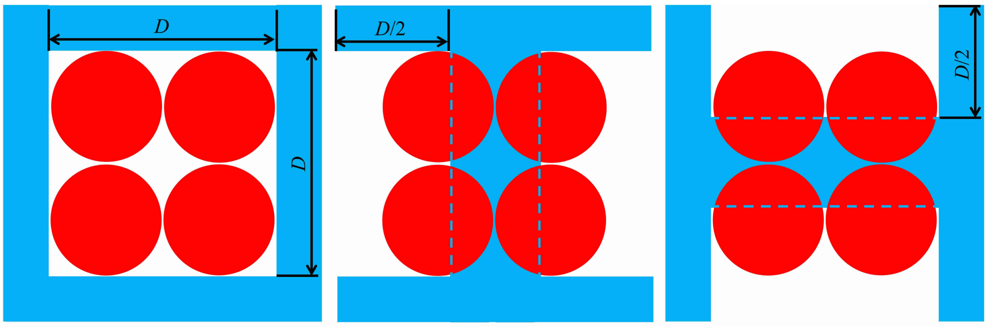

(a) L1-Center (b) L2-Horizontal (c) L3-Vertical

Figure 7: Three kinds of initial positions of particles.

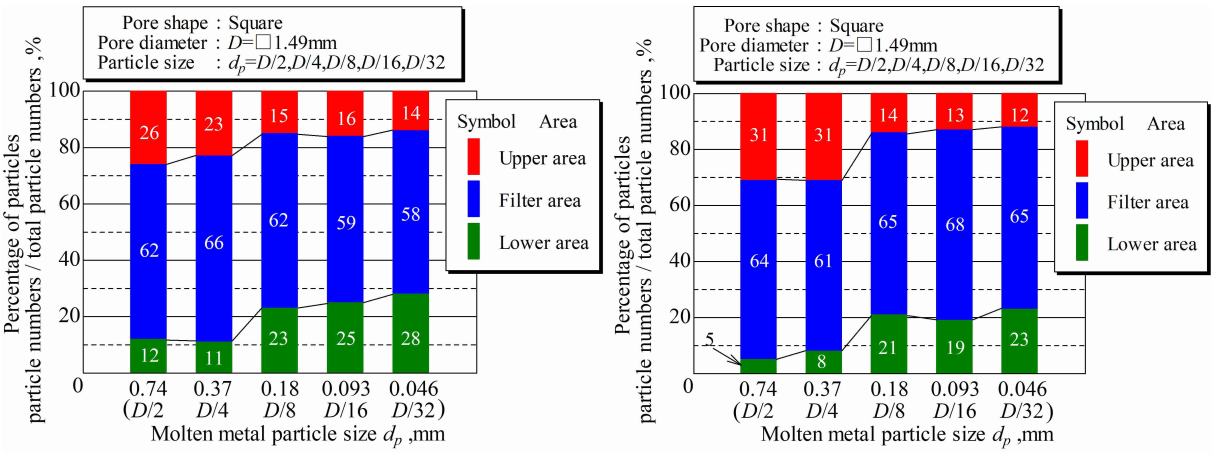

(b) L2-Horizontal (c) L3-Vertical

Figure 8: Effect of particle size on filter performances obtained by using the 1/4 model filter.

Referring to the results of K. Taki et al.[8], the mold filling simulation is possible to do using a particle size of 1mm. However, the results are a little unsatisfactory and need to be improved. The condition needs $dp =< D/16$. Under this satisfying condition, the filter pore size D needs to be modified to 16mm or more, which is not a suitable means.

Therefore, the application of a 1/2 scale casting plan and the 1/4 model filter is proposed shown in Figure 9. This casting plan is scaled down based on the 1/4 model filter, so it is called the 1/4 model for casting plan, again.

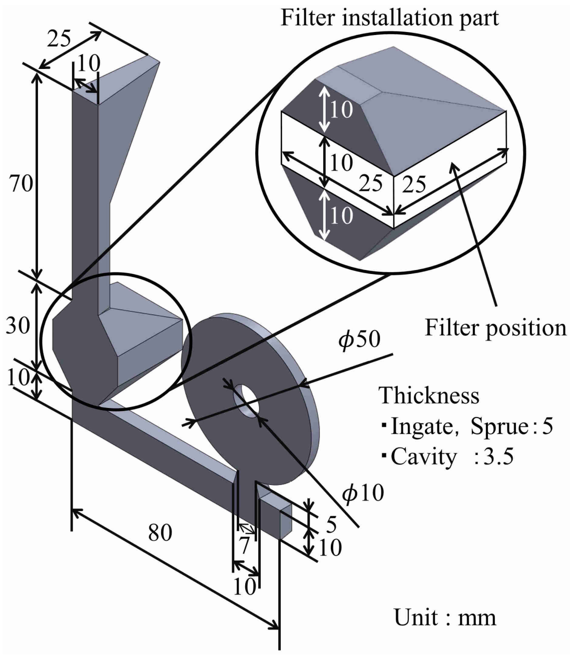

Figure 9: Overview of 1/4 model for casting plan.

4.2 Simulation using 1/2 scale casting plan

Figure 10 shows the comparison of the mold filling behaviors between the experiment and the simulated result obtained by using the 1/4 model when a strainer filter of 20t is installed. Also, Figure 11 shows the comparison of flow behaviors between the experiment and the simulated result obtained by using the 1/4 model during passes through a strainer filter 20t. The mold filling behaviors in Figure 10 and the flow behaviours during passes through a strainer filter in Figure 11 are roughly in agreement to experiment, and it is judged to be a reasonable result under the current computer environment.

5 CONCLUSION

The 1/4 model of the cast filter is proposed to simulate the mold filling behaviour. By adopting the particle size of $dp = D/16$ of the filter pore size D, the flow simulation during passes through the filter can be performed. Furthermore, in addition to the 1/4 model of the casting filter, a scaled-down model of the casting plan can be used to simulate the entire system.

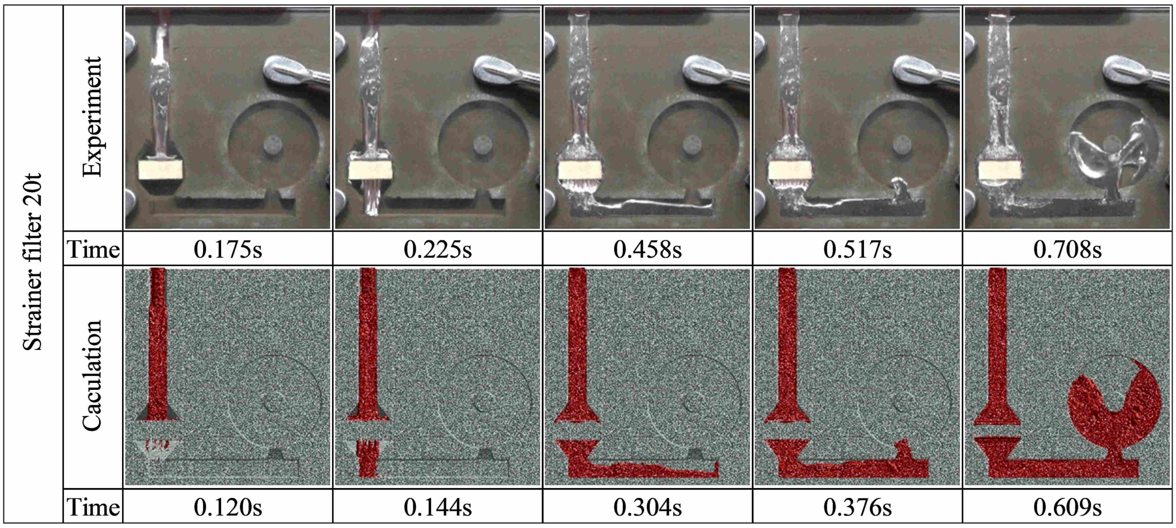

Figure 10: Comparison of the mold filling behaviors between experiment and simulated result for the 1/4 model casting plan with a strainer filter 20t.

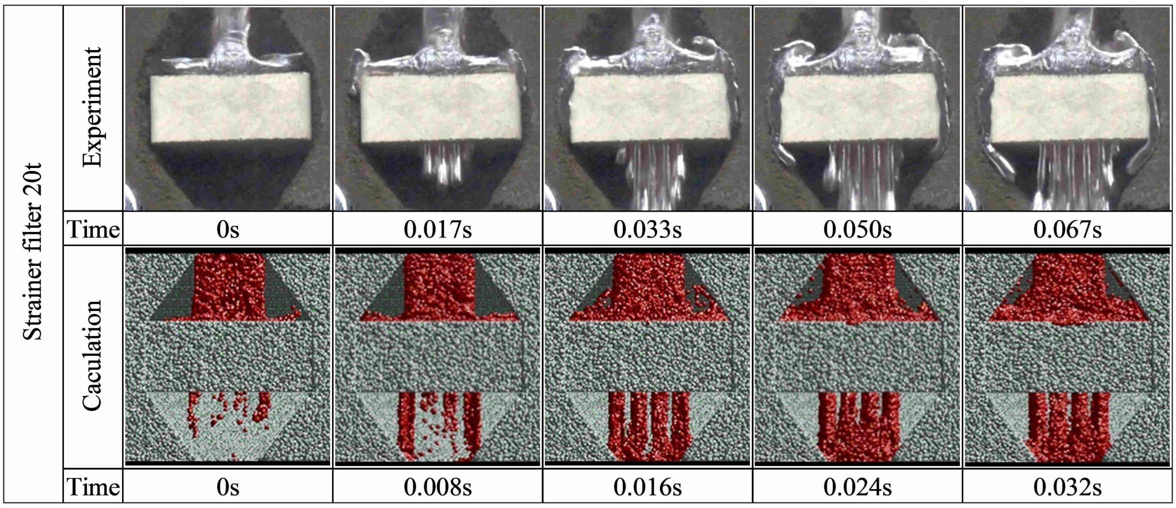

Figure 11: Comparison of flow behaviors during passes through a strainer filter 20t between experiment and simulated result for the 1/4 model casting plan.

REFERENCES

[1] Fu-Yuan-Hsu, Cheng-Lung Li. Runner Systems Containing Ceramic Foam Filters Quantified by "Area Normalized" Bifilm Index Map. *Int. J. Metalcasting*, (2015) **9**, 23-35 DOI: https://doi.org/10.1007/BF03355620

[2] S. Chakraborty, R. J O'Malley, L. Bartlett and M. Xu. Removal of Alumina Inclusions

from Molten Steel by Ceramic Foam Filtration. *Int. J. Metalcasting*, (2021) **15**, 1006-1020 DOI: https://doi.org/10.1007/s40962-020-00537-9

[3] S. Chakraborty, R. J. O'Malley and L. Bartlett. Ceramic Foam Filter Micropores as Sites for Liquid Inclusion Retention. *Int. J. Metalcasting*, (2022) **16**, 20-34 DOI: https://doi.org/10.1007/s40962-021-00585-9

[4] Y. Yang, H. Nomura, M. Takita, Y. Maeda. Effect of Filter on Flow Behavior and Inclusion Removal During Pouring. *J. Japan Foundry Engineering Society*, (1997) **69**, 62-68 DOI: https://doi.org/10.11279/jfes.69.62

[5] Jonas Bäckman, Ingvar L. Svensson, Y. Maeda. Influence of filter on the mould filling of aluminium melts in vacuum-sealed moulds. *Research Report 99:6, Division of Component Technology, The School of Engineering, Jönköping University*, **ISSN 1404-0018**, (1999)

[6] Y. Otsuka. Experimental Verification and Accuracy Improvement of Inclusion and Shrinkage Defect Simulation in Die Casting Process. *J. Japan Foundry Engineering Society*, (2013) **85**, 92-98 DOI: https://doi.org/10.11279/jfes.85.92

[7] Japan Foundry Engineering Society. *Japan Foundry Engineering Society Research Report* **No.113**, (2014) 43-47

[8] K. Taki, G. Endo and Y. Maeda. Molten Aluminum Alloy Flow through Casting Filter Installed at Sprue, *J. Metalcasting*, Online (2023). DOI: https://doi.org/10.1007/s40962-023-00976-0.

[9] M. Kazama, T. Suwa, Y. Maeda. Modeling of Computation of Molten Aluminum Alloy Flow with Oxide Film by Smoothed Particle Hydrodynamics, *J. Japan Foundry Engineering Society*, (2018) **90**, 68-74 DOI: https://doi.org/10.11279/jfes.90.68.

[10] M. Kazama, T. Suwa and Y. Maeda. Modeling and Computation of Casting Process by Particle Method, *J. Materials Engineering and Performance* (2019) **28**, 3941-3949 DOI: https://doi.org/10.1007/s11665-019-03979-3

ACKNOWLEDGMENT

The authors would like to thank Dr. M. Kazama and Dr. T. Suwa at Fujitsu Limited their technical support of COLMINA CAE.